Combination of acoustic trapping and impedance spectroscopy for platelet analysis

Carl Johannesson & Ellen Persson

2014

LUND UNIVERSITY

Master´s Thesis

Faculty of Engineering LTH
Department of Biomedical Engineering

Supervisor: Mikael Evander

Examiner: Johan Nilsson

Abstract

A combination of acoustic trapping and impedance spectroscopy for micrometer-sized objects is here presented for the first time. Acoustic trapping has proven to be a well-functioning method for non-contact immobilization and positioning of particles or cells in microfluidic channels. The combination with impedance spectroscopy allows for simultaneous electrical measurements on the trapped objects. Silica (8 μm) and polystyrene particles (3, 7, 10, and 12 μm) in saline solution, as well as human platelets in TAB buffer, have been trapped and measured. Both the saline and buffer solution had a base impedance magnitude of ~500 Ω at the utilized frequency range (100 kHz–5 MHz). The impedance magnitude for the trapped particles was ~30 Ω higher than the base impedance magnitude for the saline solution at 100 kHz–15 MHz. For the platelets, the impedance magnitude was ~60 Ω higher compared to the buffer at 100 kHz. Furthermore, the setup can be used for studies on the reaction of a trapped cluster of objects, for example cells, when the environment is changed. One way of changing the environment would be to introduce drugs in different concentrations into the channel. However, the electrical characteristics of the fluid cannot be changed. An application is presented where the system is used for measurements on platelet activation. Platelets were activated by 20 μM TRAP while trapped, which yielded a reversible impedance magnitude decrease of ~15 Ω at 100 kHz. 40 μM TRAP resulted in an initial decrease of ~24 Ω and a sustained decrease of ~15 Ω at 100 kHz. The setup presented shows great potential for being developed to an analysis system for micrometer-sized objects, for example for characterization of platelet activation.

Acknowledgements

First of all we would like to express our gratitude to our supervisor Mikael Evander, for his never-ending enthusiasm and valuable assistance and feedback during this thesis work. Furthermore, we want to thank Johan Nilsson for providing us with expert advices within the field of electrical engineering. We would like to thank David Erlinge and Siv Svensson at the department of cardiology at Skåne's University hospital for sharing their expertise and providing us with blood samples. We would also like to thank Cecilia Magnusson at Clinical Chemistry, Lund University, for helping us with the FACS analysis and results interpretation. We are also very thankful to Gustav Persson for drawing CAD images of our lab equipment. Finally, we would like to thank the entire staff at the Department of Biomedical Engineering for always being prepared to help and share their knowledge with us.

Contents

1 Introduction

For the past years, micro system technology has been increasingly integrated to the fields of biomedicine and biochemistry. Several techniques for separation and immobilization utilizing microfluidic phenomena have been developed. Acoustic trapping is an example of a technique that works very well in microfluidic channels; particles and cells can be immobilized without any physical contact with the objects by the means of acoustic standing waves. This allows for measurements on the trapped object, for example with impedance spectroscopy. Impedance spectroscopy is also a contactless technique, which is a commonly used tool for cell analysis. In this thesis, the combination of acoustic trapping and impedance spectroscopy in a microfluidic chip is presented for the first time. The combination of the two techniques is advantageous since it shows great potential of being develop to a fully automated analysis system, for example for platelets. Therefore, an application is also presented where the system is used for platelet activation analysis. Today, platelet analysis is labor-intensive and time-consuming and therefore the need of an automated system is an incentive for development of the presented system.

2 Main objectives of the thesis

The main purpose of this thesis was to develop a method for simultaneous contactless acoustic trapping and impedance measurement for particles and cells. Since acoustic trapping normally is used for particles ranging between 1 and 20 µm [1], this was the targeted dimension range also in this project. A more specific objective of the project was to evaluate whether the methods of trapping and impedance measurement can be used for platelets, which are highly important blood components for hemostasis, i.e. prevention of blood loss. Below follow the main questions that have been investigated during the project.

I. Is it possible to simultaneously perform acoustic trapping and impedance spectroscopy?

II. Is it possible to combine acoustic trapping and impedance spectroscopy for polystyrene and silica particles?

III. Is it possible to combine acoustic trapping and impedance spectroscopy for platelets?

IV. Is it possible to hold the platelets in the trap without activating them?

V. Is it possible to differ activated from non-activated platelets by using the combination of acoustic trapping and impedance spectroscopy?

3 Background

3.1 Techniques available for micro particle trapping

Immobilization of micrometer-sized objects is a helpful method within numerous life science research areas. Microscopy studies, enrichment of cells from dilute suspensions and studies on cell-cell interactions, which is the area of application in this thesis, are examples of applications that can be simplified by means of trapping.

In addition to acoustic trapping, which is the technique used in this thesis, several different techniques for particle and cell trapping exist, and many of them can be implemented in microfluidic chips. The techniques utilize different forces, for example hydrodynamic, optical, dielectrophoretic, and magnetic forces. Each technique has different limiting factors, and they are therefore not directly interchangeable. Optical technologies demand transparent buffers, and dielectrophoretic methods can only handle buffers with certain pH and ion concentrations. Magnetic trapping demands a buffer that differs in magnetism from the particles that should be trapped. This is a problem when cells should be trapped. Acoustic techniques, however, only demand a buffer that differs in density and/or compressibility relative to the particles, which is the case for basically all buffers. Hydrodynamic trapping has no buffer requirements. Depending on whether single cells or cell clusters should be trapped, different methods are preferred. Optical trapping is more adequate for single cell trapping, while acoustic trapping is suitable for cell clusters [2].

3.2 Advantages of lab-on-a-chip for life science analysis

Development of miniaturized analysis systems, so called lab-on-a-chip, within the field of life science is a growing research area and highly integrated micro devices have the opportunity to enhance this research. Many advantages come with downscaling the size of the devices. First, the spatial and temporal microenvironment for a cell can be more precisely monitored and modulated in a micro system than in a macro system. The reason for this is the predictable

behavior of fluids in micrometer-sized channels and the ability to modify the surfaces in contact with the fluid to be analyzed. This enables a more *in vivo*-like environment. Second, higher throughput is more easily accomplished with micro-fabricated analysis systems, because several probing systems can be run in parallel, and this gives a better statistical foundation. Third, the spacing between cells can be more carefully controlled compared to traditionally used cell cultures, and this allows for single-cell studies and more advanced cell-cell interaction studies. Last, micro analysis systems reduce the reagent consumption and smaller sample volumes of, for example cell cultures, are needed [3].

4 Theory

4.1 Microfluidics

Studies on the behavior of small volumes of fluids, e.g. droplets, jets, thin water films or fluids in micro channels, lie within the field of microfluidics. *Small* can, in this case, be defined as something that, in at least one dimension, is smaller than 1 mm. Fluids on this scale behave in a different way compared to fluids on the macro scale. Other forces, than those dominating on the macro scale, are very important for the behavior of a fluid on the micro scale. Gravity is, for example, not as important as viscous forces and surface tension [3]. Below follows a description of phenomena important within microfluidics.

4.1.1 Laminar flow

Fluids flowing in a micro channel behave differently to the same fluids flowing in a macro system; the flow on the micro scale is usually laminar, whereas on the macro scale it is usually turbulent. Laminar flow is advantageous when doing acoustic trapping and is only achieved if the Reynolds number of the fluidic system is low enough. Laminar flow means that the streamlines in the channel are parallel to each other and that no mixing occurs, except for diffusion, which is always present. Turbulent flow is characterized by three-dimensional vortex motions although the bulk flow is in one dimension [3]. See *Figure 4.1* for a comparison between laminar and turbulent flow. The flow pattern anticipated in a system can be calculated by the Reynolds number, *Re*, which is given by *Equation 1*.

$$Re = \frac{\rho u L}{\eta} = \frac{u L}{\nu} \qquad [1]$$

where ρ is the density of the fluid, u is the average flow speed, L is a length scale characteristic of the flow (for example the diameter of a cylindrical channel), η is the dynamic viscosity, and ν is the kinematic viscosity. The Reynolds number is a measure of the ratio between inertial forces and viscous forces in a flow. If the number is below 2000 the flow is usually laminar, whereas a system with a number above 2000 is more likely to have a turbulent flow. In general the Reynolds number in microfluidic systems is below 0.1. Thus, the flow is strictly laminar. In addition to being beneficial for acoustic

trapping, laminar flow is advantageous from a simulation perspective, since it can be mathematically modeled [3].

4.1.2 Parabolic flow profile

Laminar flow creates a parabolic flow profile. This means that the fluid flows faster in the center of the channel than at the channel walls. This is usually explained by the no-slip condition, which states that the flow velocity of the fluid at the walls is zero, see *Figure 4.1* for a schematic image of parabolic flow profile [3].

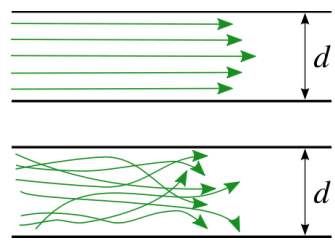

Figure 4.1. The top image shows laminar flow and the bottom image shows turbulent flow. The top image also shows a parabolic flow profile; the fluid velocity is higher in the middle than further to the sides [4].

4.1.3 Stokes drag

A spherical particle at rest in a fluid moving past it, or a particle moving in a fluid at rest, will be subjected to a force called Stokes drag, F_{drag}, which under laminar flow conditions and when there is no interaction between different particles is given by *Equation 2*.

$$F_{drag} = 6\pi\eta a v \qquad [2]$$

where η is the dynamic viscosity, a is the radius of the sphere, and v is the fluid velocity compared to the particle. The force acts in the same direction as the direction of the fluid flow relative to the particle [5]. The drag force is important to compare with trapping forces emerging when an acoustic field is applied to a fluid containing particles, since the drag force is counteracting some of the trapping forces [6], which are explained in *Section 4.2.2 Acoustic forces*. See *Figure 4.2* for an illustration of Stokes drag force.

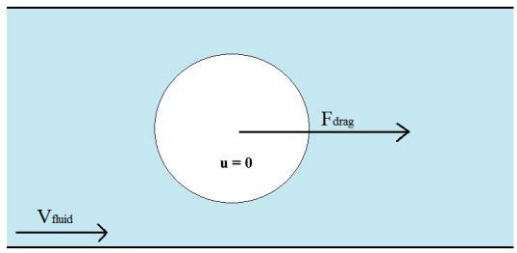

Figure 4.2. Stokes drag acting on a particle standing still in a fluid moving past the particle. *u* is the particle speed. The force is acting in the direction of the fluid flow.

4.2 Acoustofluidics

Acoustofluidics refers to microfluidic systems, for example a micrometer-sized channel, in which acoustic pressure fields are applied. The applied sound waves can form standing waves in the micro channel. If the right frequency is applied, the standing wave can be used to manipulate, for example sort or trap, particles and cells contained in a fluid [5]. One type of acoustic manipulation is acoustic trapping, which is a central theme of this thesis.

4.2.1 Principles of acoustic trapping

Acoustic trapping is a non-invasive and contactless method for immobilization of small objects by utilization of forces arising when an ultrasound field is imposed on a fluid in a channel. These forces can even be strong enough to hold one or several objects in place against a fluid flow. Usually, the method is used for particles or cells with a diameter ranging from 1 to 20 µm. Several acoustic forces contribute to trapping and the properties of these forces depend only on the geometrical dimensions and material characteristics of the trapping system. Hence, trapping takes place independently of properties like pH-value, ionic strength of the fluid, and surface charge, which are all limiting properties of other trapping techniques, see *Section 3.1 Techniques available for micro particle trapping*. It is difficult to trap particles smaller than 1 µm in diameter since the major trapping force, the primary radiation force, is not large enough to counteract the flow drag at small object volumes, *see Equation 5*. If the particles are too large, approximately 20 µm in diameter, the gravitation could become too dominant, depending on the density of the object compared to the fluid, and thereby decrease the trapping efficiency [1, 6-8].

For trapping to occur, an acoustic wave field, i.e. ultrasound, has to be generated in the fluid channel. The acoustic wave field, which is mechanical waves propagating in a fluid, can be created by a piezoceramic transducer brought in close contact with the microfluidic channel. If the acoustic impedance, see *Section 4.2.7 Acoustic impedance*, is properly matched, the vibrations will reach the fluid of the channel and if a resonance criterion of the channel is met, a standing wave will form [6]. The standing wave can for example be formed between the side walls of the channel or between the top and bottom [9]. There are several resonance criterions, of which one has to be fulfilled. The half wavelength-criterion is the most commonly used resonance criterion and it is fulfilled if the width, *w*, or height, *h*, of the channel is

$$w = \frac{v}{2f} = n\frac{\lambda}{2} \qquad [3]$$

where *v* is the speed of sound in the fluid, *f* is the acoustic frequency, *n* is the number of pressure nodes in the standing wave, and λ is the wavelength of the sound. *Figure 4.3a (side view)* shows a λ/2-standing wave. One or several pressure nodes can be created in the channel. The number of nodes depends on the operating frequency of the transducer, and thus the resonating frequency of the whole resonating system, i.e. the microfluidic chip with fluid, transducer, and holder [1, 10]. When *n* = 1 in the half wavelength-configuration, there will be one pressure node in the channel and it will be located at the center of the channel. If the particles have higher density or lower compressibility than the fluid, the trapping forces collect the particles to the pressure node/-s, see *Figure 4.3b (top view).*

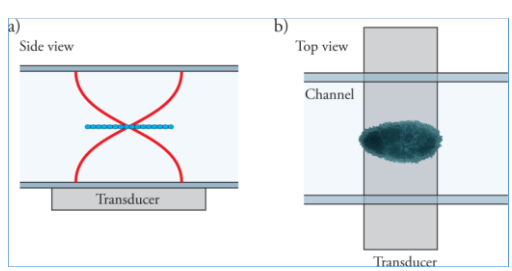

Figure 4.3. The side view (a) shows a λ/2-standing wave with one pressure node between the top and bottom of the channel. The top view (b) shows a trapped cluster of particles at the pressure node right above the transducer. Reproduced from [11] with permission of the author.

In order to create a well-functioning acoustic trap, the acoustic resonance should be located only in a small part of the channel, at the site where trapping is desired. This can for example be achieved by bringing the transducer in close contact with the microfluidic chip and placing it at the point of the channel where trapping is desired. This will lead to a steep acoustic gradient, which gives efficient trapping, i.e. strong trapping forces [1].

4.2.2 Acoustic forces

Several forces are contributing to the immobilization of particles suspended in a fluid during acoustic trapping. First and foremost, a primary acoustic radiation force, F_{rad}, originating from the standing wave, affects particles or cells being trapped. It can be expressed as the gradient of the acoustic potential, U_{rad}, given by *Equation 4.*

$$F_{rad} = -\nabla U_{rad} \quad [4]$$

Simplification of F_{rad} to one dimension gives the *axial* acoustic radiation force, F_{axial}. For a planar standing λ/2-wave, F_{axial} is given by *Equation 5.*

$$F_{axial} = 4\pi R^3 E_{ac} \Phi\, k \sin(2kx) \quad [5]$$

where R is the particle radius, E_{ac} is the acoustic energy density, Φ is the acoustic contrast factor, see *Equation 6*, k is the wavenumber, see *Equation 7*, and x is the particle position in the wave propagation direction.

$$\Phi = \frac{\rho_p + (2/3)(\rho_p - \rho_0)}{2\rho_p + \rho_0} - \frac{1}{3}\frac{\rho_0 c_0^2}{\rho_p c_p^2} \quad [6]$$

$$k = \frac{2\pi f}{c_0} \quad [7]$$

where ρ_p and ρ_0 are the densities of particle and fluid respectively, c_p and c_0 are the speed of sound in the particle material and fluid respectively, and f is the frequency of the standing wave. The primary radiation force is the strongest acoustic force, but since the magnitude depends strongly on the particle size, the force decreases rapidly with decreasing particle volume. The force scales with the cube of the radius [6, 12]. Another important relationship is the proportionality between the magnitude of the force and the frequency

utilized for the ultrasound generation. This is one reason to why acoustic trapping works so well in microfluidic devices. In micro channels, a higher frequency is required for standing waves to arise and a higher frequency results in a larger trapping force, see *Equations 5* and *7* [1].

Particles subjected to the trapping forces will move either to the point where the acoustic potential is at its maximum or where it is at its minimum, depending on the compressibility and the density of the particle to be trapped with respect to the fluid. In the case of a perfect standing wave, the point of minimal acoustic potential coincides with the pressure node, i.e. the point of lowest pressure. If the density of the particle is higher and/or the compressibility lower, compared to the fluid, the particle will move to the pressure node [6], see *Figure 4.4a* and *b* for schematics of the primary radiation force. For instance, when trapping cells in a saline solution, the cells will be trapped at the pressure node (if assuming a perfect standing wave) since the density of the cells is higher than that of the fluid.

Acoustic trapping also relies on a secondary radiation forces, also called Bjerknes forces, emerging due to scattering of the acoustic waves when multiple particles are in close proximity. Since the secondary radiation force attracts the particles within the pressure node towards each other, the force provides stabilization to the trapped particle cluster and promotes further clustering [6, 12]. See *Figure 4.4c* for a schematic of the secondary radiation force.

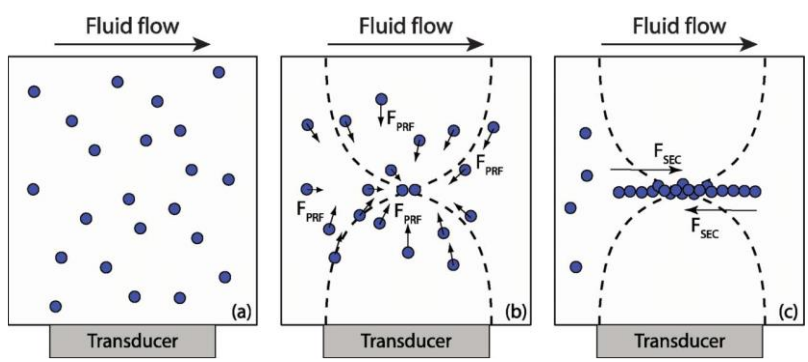

Figure 4.4. The schematics show particles being trapped at the pressure node by primary (PRF) (b) and secondary (SEC) (c) acoustic radiation forces. The primary forces bring the particles into the node and the secondary forces stabilizes the cluster. Reproduced from [6] with permission of The Royal Society of Chemistry.

Stokes drag force, which was mentioned in *Section 4.1.3 Stokes drag*, is counteracted by the lateral component of the primary radiation force. While the axial component works in the direction of the primary acoustic wave field propagation, the lateral component is perpendicular to the primary acoustic wave direction. The lateral component is smaller than the axial, but still strong enough to withstand the drag from the passing fluid [6].

4.2.3 Resonator design

The resonator consists of a microfluidic chip with a fluid-containing channel, a transducer, and coupling layers between them. Different designs of resonators exist, for example the layered resonator in which the different layers are matched with regard to type of material and thickness [1]. A layered resonator generates a standing wave in the direction of the sound propagation. In order to get a well-functioning resonator, it is beneficial if the thicknesses of the layers are made according to the criteria given in *Figure 4.5* [1].

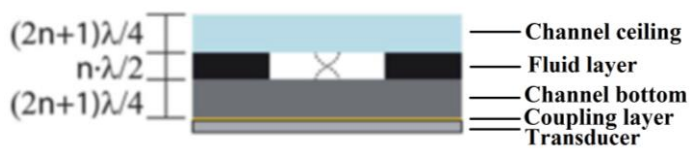

Figure 4.5. Schematic of a layered resonator with the theoretically favorable thickness criteria marked. Reproduced from [1] with permission of The Royal Society of Chemistry.

4.2.4 Piezoelectric transducer

The piezoelectric transducer is the part of the resonator generating the ultrasound, i.e. the mechanical waves that are transmitted into the channel fluid. When a piezoelectric material is subjected to mechanical strain, an electric potential gradient is created in the direction of the applied stress. Converse piezoelectricity is due to the opposite reaction; when an electrical field is applied over the piezocrystal, mechanical strain is generated. By using an alternating voltage, the piezocrystal will start to oscillate at the frequency of the applied voltage [11].

The transducer's dimensions govern the efficiency of energy transmission to adjacent resonator layers. According to Glynne-Jones et al., the thickness of the piezocrystal has to be close to ~0.84*λ/2 in order to get maximum acoustic energy transmitted into the microfluidic channel, and consequently obtain a standing wave that can be used for trapping [10].

4.2.5 Kerfed transducer

The dimensions of the piezoceramic transducer determine its vibrational resonance frequency. In order to create a well-functioning acoustic trapping system, it is important that the vibrational resonance arising from the thickness of the transducer differs from the resonance of the other geometrical dimensions. A kerfed transducer, i.e. a transducer that has been cut to form thin ridges in the length direction, can be used to achieve this. *Figure 4.6* shows a kerfed transducer. The ridges lead to a higher resonance frequency in the width direction than the transducer would have without the ridges. Therefore, the frequency originating from vibrations in the width direction will not interfere with the frequency originating from the thickness direction, which is the utilized frequency [13].

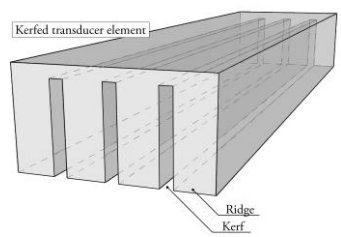

Figure 4.6. Schematic of a kerfed transducer. The ridges are sawed since it prevents the frequency originating from vibrations in the width direction from interfering with the utilized thickness frequency. Reproduced from [11] with permission of the author.

4.2.6 Q-factor

The resonance property of an acoustic resonator can be described by the unitless quality factor, *Q*, also called Q-factor or Q-value. It describes the bandwidth of the sound waves generating resonance in the system [14]. It can be calculated by *Equation 8.*

$$Q = \frac{f_0}{\Delta f} = \frac{f_0}{f_u - f_l} \qquad [8]$$

where f_0 is the resonance frequency, Δf is the bandwidth of the resonance peak, f_u is the upper frequency, and f_l is the lower frequency, i.e. f_u and f_l are the borders of the bandwidth. The center frequency is the least damped frequency, i.e. the resonance frequency that transmits the most acoustic energy to the channel. Broad bandwidths give low Q-factors and narrow bandwidths give high Q-factors. A high Q-factor implies that the system has low attenuation of the mechanical waves [14, 15]. However, the system is more

sensitive to temperature changes if the value is high. Therefore, in acoustofluidics these factors have to be weighed against each other when designing the system.

4.2.7 Acoustic impedance

The characteristic acoustic impedance, Z, of the resonator materials is an important factor for how well the resonator works and traps objects. When an acoustic wave travels through one medium and encounters a second medium, the wave is partly transmitted and partly reflected. How much of the energy that is reflected and how much is transmitted depends on the acoustic impedances of the two media [1]. The acoustic impedance is given by *Equation 9.*

$$Z = \rho c \qquad [9]$$

where ρ is the density and c the speed of sound in the material [1]. The pressure reflection coefficient, R_p, is calculated by *Equation 10.*

$$R_p = \frac{Z_2 - Z_1}{Z_1 + Z_2} \qquad [10]$$

where Z_1 is the characteristic acoustic impedance of the first medium and Z_2 of the second [1]. The pressure transmissions coefficient, T_p, is calculated by *Equation 11*.

$$T_p = 1 - R_p \qquad [11]$$

To establish a well-performing trapping system it is important that the greater part of the acoustic energy is transmitted from the transducer into the channel fluid and maintained there [1]. This is accomplished by choosing materials with respect to their acoustic impedances. Where transmission is wanted, the second material should have lower acoustic impedance than the first material, and where reflection is wanted, vice versa.

4.2.8 Flow channel material

Acoustophoretic devices have been manufactured from many different materials. The most frequently used fluid channel material is silicon [8]. It is an advantageous material since it can be precisely structured using etching techniques; with wet and dry etching one can accomplish channels with

vertical walls, which is commonly used in standing wave acoustics. Glass is an alternative to silicon. The fabrication methods for glass channels are usually less complicated and cheaper than for other materials, for example silicon. Further advantages of glass are the transparency, the high speed of sound in the material and the larger density compared to aqueous fluids that gives higher acoustic impedance compared to aqueous fluids. In addition, glass has low acoustic attenuation and is chemically inert, which is necessary when for example working with biological samples [1, 9].

4.3 Impedance spectroscopy

When a voltage is applied to an electrical circuit, a current is generated and it will encounter a certain opposition in the circuit; this is the electrical impedance. When a direct voltage is applied, the impedance will only have a magnitude. The impedance is in this case often called resistance. If an alternating voltage is applied, the current will have a phase shift relative to the voltage and consequently, the impedance will have both magnitude and phase, see *Figure 4.7*. Impedance spectroscopy is a technique used to measure the impedance at different frequencies of the applied voltage. A range of frequencies is used and the impedance is plotted against the frequency [16, 17].

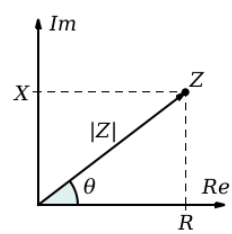

Figure 4.7. Impedance have magnitude ($|Z|$) and phase (θ) [18].

4.4 Cells in electrical fields

When an electrical field is applied over a cell solution the current takes different paths through the solution depending on the frequency of the applied alternating voltage. Due to this, different frequencies give different information about the cells and the frequencies are divided into three dispersion ranges: α-, β- and γ-dispersion. At low frequencies (1 Hz–100 kHz), the α-dispersion range, the cell membrane acts as a barrier and the current only

passes through the surrounding solution. The frequency at which the membrane lets current through is known as the β-relaxation frequency, which lies within the β-dispersion range. The β-relaxation frequency is normally a few MHz and the current is able to pass through the membrane since membrane polarization decreases with increasing frequency.

β-dispersion can be explained by modelling the membrane as an electrical capacitor, consequently low frequency currents cannot pass through the membrane since the impedance magnitude is too high. However, if the frequency is increased, the impedance magnitude of the cell membrane decreases and the current can pass through the membrane and the inner of the cell, see *Figure 4.8*. The higher the frequency, the lower the impedance magnitude. The solution surrounding the cells, as well as the intracellular fluid, can be electrically modeled as resistances, which are independent of the frequency, see *Figure 4.8* for an equivalent circuit diagram of cells and the surrounding solution [19-22].

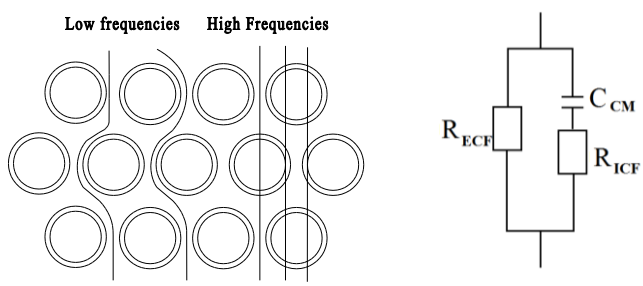

Figure 4.8. The left figure shows the paths of low and high frequency-currents through a cell suspension. Low frequencies are blocked by the membranes and only pass through the solution surrounding the cells, while high frequencies pass through the cell membranes and the intracellular fluid. The right figure shows the equivalent circuit diagram of cells and the surrounding fluid. R_{ECF} corresponds to the resistance of the extracellular fluid, R_{ICF} is the resistance of intracellular fluid, and C_{CM} is the capacitance of the cell membrane.

4.5 Platelets

Platelets play a vital role in the prevention of blood loss, also called hemostasis [23]. They are also called thrombocytes and contribute to the process of hemostasis in many different ways. An important part of hemostasis is the activation of platelets. Deficiency or malfunctioning of platelets as well as pathophysiological activation can be life threatening [23, 24]. Platelets affect diseases like thrombosis, vessel constriction, atherogenesis, tumor growth and metastasis and atherosclerosis [25].

4.5.1 Physical characteristics

Platelets are blood components circulating throughout the whole body. They are normally discoid, measure 3.0 × 0.5 µm in diameter, and have a mean volume of 7–11 fL (femtoliter). A healthy person has 150 000–400 000 platelets per µL of blood [26]. See *Figure 4.9* for a size comparison of platelets to other blood components.

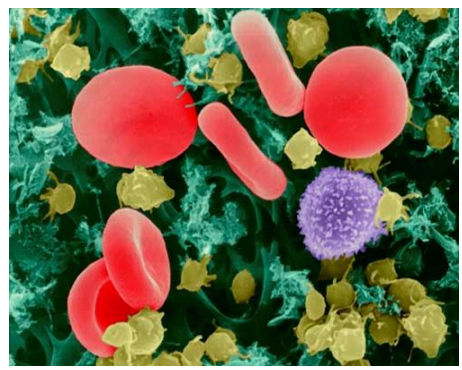

Figure 4.9 Scanning electron microscope (SEM) image of platelets (yellow), red blood cells (red), and a small white blood cell (purple). Image courtesy of M.D. David Erlinge, Department of Cardiology, Lund University.

Platelets are strictly speaking not cells, but have functional resemblances to cells. First, the cytoplasm is filled with contractile proteins called actin, myosin and thrombosthenin, and the platelet can therefore quickly change shape, which happens during activation. Second, like any regular cell, platelets have mitochondria that produce adenosine diphosphate (ADP) and adenosine triphosphate (ATP). In addition, they have residuals of endoplasmic reticulum and Golgi apparatus, which synthesize and store large quantities of calcium ions needed in hemostasis [23].

The inner of the platelets, the cytoplasm, is filled with three types of storage granules: dense granules, α-granules, and lysosomes. α-granules are the most abundant ones and contain clotting factors, von Willebrand factor (vWF), platelet-derived growth factor (PDGF) and other proteins. Dense granules are filled with ADP, ATP, serotonin and calcium. Hydrolytic enzymes are stored in the lysosomes. All these molecules contained in the granules are ejected from the platelets when they are being activated [26].

4.5.2 Hemostasis and platelet function

Whenever a blood vessel is ruptured or damaged, a series of events takes place to prevent blood loss. Platelet activation plays a vital role in the process, and it ultimately leads to formation of a mechanical platelet plug at the source of the hemorrhage. When platelets reach an area where the vascular surface, endothelium, has been injured the platelets immediately react by a series of physical changes. They swell and change form to compact spheres with projections, pseudopods, irradiating from their surfaces [27]. *Figure 4.10* shows images of non-activated and activated platelets. Myosin and actin cause the platelets to contract and release granules with factors necessary for further hemostasis steps. Adhesion of platelets to the vessel wall, especially to the collagen fibers in the wall, and aggregation of platelets (platelet-platelet adhesion) takes place since the surface of the platelets becomes sticky upon activation. Discharge of ADP and thromboxane A_2 starts a positive feedback loop by acting on nearby platelets and activating them, so that they become sticky and adhere to platelets already anchored at the vessel wall. The positive feedback loop will eventually lead to formation of a platelet plug. This plug is enough to stop the bleeding if the damage is small. Minute ruptures occur throughout the vascular system many thousands of times every day and the platelet plugs are extremely important for healing these [23, 26].

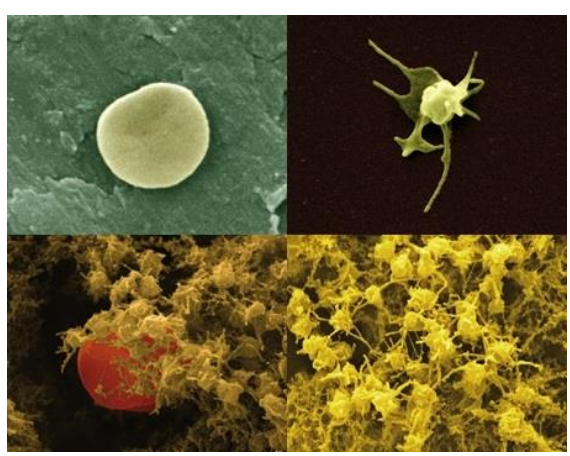

Figure 4.10. Scanning electron microscope (SEM) images of platelets. The two top images show a non-activated (left) and an activated (right) platelet. The bottom images show activated platelets connecting to each other (left and right) and to a red blood cell (left). Image courtesy of M.D. David Erlinge, Department of Cardiology, Lund University.

4.5.3 Reversible activation

Aggregation can be reversible, i.e. a platelet aggregate can dissolve if it is unstable. These non-stable aggregates are formed when platelets, which have not yet gone through a full shape change, link to each other via long membrane tethers. Membrane tethers are cylinders of lipid bilayer that are pulled from the surface of platelets under the influence of hemodynamic drag force [28]. An irreversible aggregate consists of fused platelets and the original membrane structure from the individual platelets has vanished. The release from the granules is more intense when an irreversible aggregation takes place compared to a reversible [29]. A stable aggregation phase follows subsequent to the reversible aggregation phase [28].

4.5.4 Shear stress-induced activation

Platelets can become activated if subjected to high shear stress. This can for example happen in the body if an artery is obstructed by an atheromatous plaque. Studies have shown that platelet activation markers like platelet count, plasma serotonin concentration, and platelet P-selectin expression all show significant changes when human blood has been exposed to high shear stress of 20 and 30 Pa [30]. Shear stress-induced activation can pose a problem when doing activation studies on whole blood or enriched platelets, and when blood is in contact with medical devices.

4.6 Techniques for platelet measurements

The technique developed in this project was tested on platelets. Therefore, a summary of some of the testing methods available today for studies on platelets is presented below.

4.6.1 Platelet aggregometry

Platelet aggregometry is one example of a frequently used technique where the aggregation in whole blood or in platelet-rich plasma (PRP) is evaluated in response to an agonist, for example ADP or collagen [29, 31]. Light transmission aggregometry, also called Born aggregometry, is the traditional form of aggregometry and measures the light transmission change due to aggregation in blood plasma. There are also aggregometers that measure the changes in electrical resistance in whole blood due to adhesion and aggregation [31]. These aggregometers are better than the light transmission

aggregometers, mainly because they can be used with whole blood, but also because they can be combined with ATP luminescence measurements, which gives information on the granule content release [32].

It is important to point out that the aggregate formation that is observed *ex vivo* is not directly corresponding to the aggregation *in vivo*. First, because the process of acquiring the blood sample from the body is highly likely to induce shape change of the platelets. Second, because the environment outside of the body is different from the one inside, for example pH and temperature often differ. Moreover, different agonists will lead to different reactions and the aggregation results are therefore not directly comparable. These differences have to be taken into account when assessing an aggregometry test. Furthermore, aggregation is not a direct measure of platelet function in hemostasis as such, but a test of the platelets' ability to interact with each other and form aggregates [29].

4.6.2 Flow cytometry

Flow cytometry, which is an alternative to aggregometry, does however directly measure the platelet function. The method determines the density of platelet membrane glycoproteins and receptors by labeling the platelets with fluorophores and measuring the light emitted from the fluorophores subsequent to laser irradiation. Some of the receptors, for example P-selectin, are only present on the surface when the platelets are active, other receptors change shape configuration whenever the platelets are activated. By measuring the intensity of the emitted light, the density of an antigen, for example a glycoprotein, can be calculated. The emission and the antigen density are directly proportional to each other and the presence of the antigens relates to the activation of the platelets [32]. Only very small volumes of blood or platelet-rich plasma are required and the cells are analyzed at a rate of 2000 cells/second [31, 32]. Flow cytometry has the advantage over light transmission aggregometry of being able to analyze whole blood, and not just platelet-rich plasma. Since whole blood needs to be less pre-treated than platelet-rich plasma, there is a lower risk of inducing activation or other changes to the platelets prior to the test. However, the blood has to be highly diluted before it can be analyzed by flow cytometry. Another advantage of flow cytometry is the ability to discover subpopulations of activated platelets; the method can detect subpopulations where only 1% of the platelets are activated [32].

4.6.3 Cell counting

A third method of estimating the function of the platelets is to count the platelets before and after addition of an agonist. In a healthy patient, there will be a lower platelet count after the agonist has been added since it should induce aggregation, and the number of freely circulating platelets will be reduced. There are several methods for counting platelets, where one is to use a coulter counter (the cells are passed through an orifice concurrent with an electrical current and every time a cell passes the orifice, there will be a change in the impedance). Just like aggregometry, this method measures the aggregation and not the actual function of the platelets [32].

4.7 Advantages of acoustic trapping and impedance spectroscopy for platelet measurements

When investigating the activation process of platelets, it can be beneficial to study a cluster of them, since platelet-platelet interactions are crucial for the process. Furthermore, as with many other studies of cell functionality, a non-contact trapping method is preferred when doing platelet measurements. If the platelets are in contact with the trapping instrument, the study fails to mimic the platelets' natural environment, which could lead to behaviors not comparable to *in vivo* situations. Acoustic techniques offer both cluster trapping and non-contact handling, and are therefore well suited for studies on platelets. They are also relatively easy to use [7].

Impedance spectroscopy also has several advantageous qualities making it suitable for platelet analysis. First, the samples do not need to be fluorescently labeled before a test can be run, which is the case for flow cytometry. Labeling is not only time consuming and expensive, but could also potentially affect the platelets' activation status [33]. A second advantage of impedance spectroscopy over other methods for platelet analysis is the possibility to perform the measurements in a microfluidic device, which has been done in this project. Consequently, the advantages of a microfluidic system can be employed, for example smaller sample volumes than what is required in aggregometry are needed for the analysis [29]. Furthermore, just as acoustic trapping, impedance spectroscopy is performed without any physical contact with the measured object and it is, as has been pointed out earlier, beneficial

when doing measurements on cells. However, the cells might be affected if high voltages are used. Additionally, the work required by biomedical analysts can be reduced significantly by combining acoustic trapping with impedance spectroscopy. The system could potentially be developed to an automated system.

5 Methods and Materials

5.1 Experimental setup

5.1.1 Overview of the setup

The experimental setup consisted of a glass chip, ultrasound transducer, chip holder (containing the glass chip and the transducer), syringe pump (SP210IWZ, WPI, Sarasota, FL), 1 and 5 mL syringes (300013 and 309649, Plastipak, BD, Franklin Lakes, NJ), fluid valve, impedance analyzer (4194A, Hewlett Packard, Palo Alto, CA), waveform generator (33120A, Hewlett Packard, Palo Alto, CA) that actuated the ultrasound transducer, microscope (SMZ-2T, Nikon, Tokyo, Japan), camera (EO-1312C, Edmund Optics, Barrington, NJ), MATLAB® R2104a (The MathWorks Inc., Natick, MA, 2014), and a frequency tracker (manufactured by M. Evander and B. Hammarström). *Figure 5.1* shows a block diagram of the experimental setup. The setup is described more thoroughly in *Sections 5.1.2-5.1.5*.

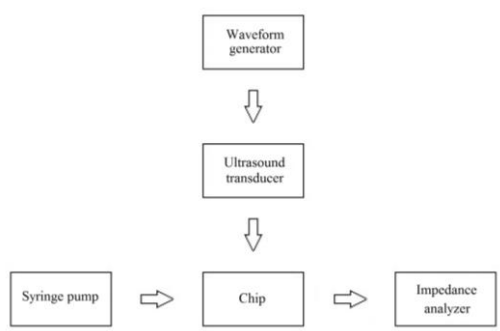

Figure 5.1. Block diagram showing the experimental setup.

5.1.2 Glass chip

Glass chips were used for the experiments in this project. They were designed by Mikael Evander and manufactured by Micronit Microfluidics B.V. The structure of the chips was designed in order to allow for simultaneous acoustic trapping and impedance spectroscopy, see *Figure 5.2* and *Figure 5.3*. The chips consisted of a three-layered structure comprising a microfluidic channel in the middle layer, where the channel was 26 mm long, 2 mm wide and 200 µm deep. In order to make it possible to see through the channel with a

light microscope, the three layers were made of borosilicate glass. Two electrodes made of platinum were positioned over and under, respectively, the trapping position in the middle of the channel, see *Figure 5.2*. They were rectangular with a finger structure, see *Figure 5.3*, and the width and length were 0.92 mm and 0.55 mm. Each finger was 0.45 mm long and 0.04 mm wide. Each electrode was connected to a contact pad further to the edge of the chip, to achieve more accessible electrode contact positions. The top electrode pad could be connected from the top side of the chip, and vice versa.

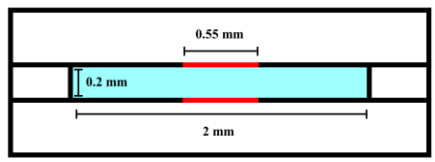

Figure 5.2. Schematic cross-section along the short side through the center of the microfluidic chip. The channel is the blue part. The red lines indicate where the electrodes are located on the glass wall inside the channel.

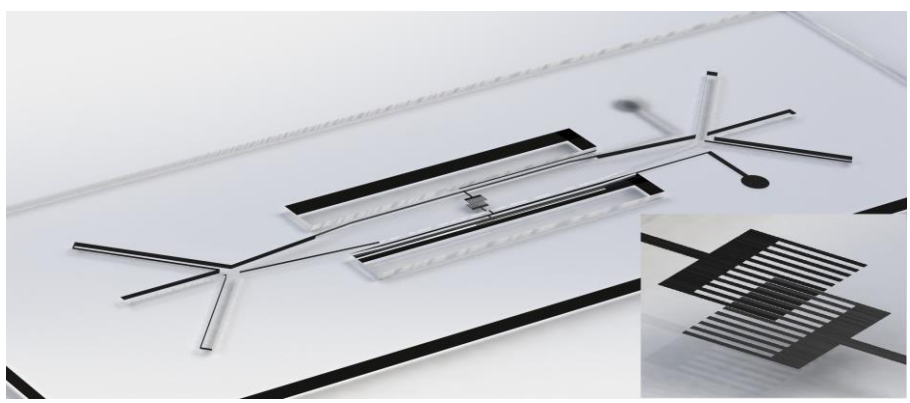

Figure 5.3. 3D-model of the glass chip showing the channel, the six inlets and outlets, and the electrodes in the center of the channel. The inserted schematic shows the electrodes, which are attached to the bottom and ceiling of the channel. Image courtesy of Gustav Persson.

Each side of the channel had three inlets/outlets, with a width of 0.5 mm. The fact that there were three inlets made it possible to pre-focus the sample fluid, so called hydrodynamic focusing, before it reached the main channel. Silicone tubing was glued to the inlets and outlets, which made it possible to connect to further tubing and syringes, see *Figure 5.4* for images of the chip. In this project, only one channel inlet was used and connected via a valve to the

syringe pump, while the rest were plugged. However, all of the three outlets were used to discharge fluid. Since a valve was used, it was possible to select and change which fluid was to go through the chip and whether particles and platelets were to be inserted or not.

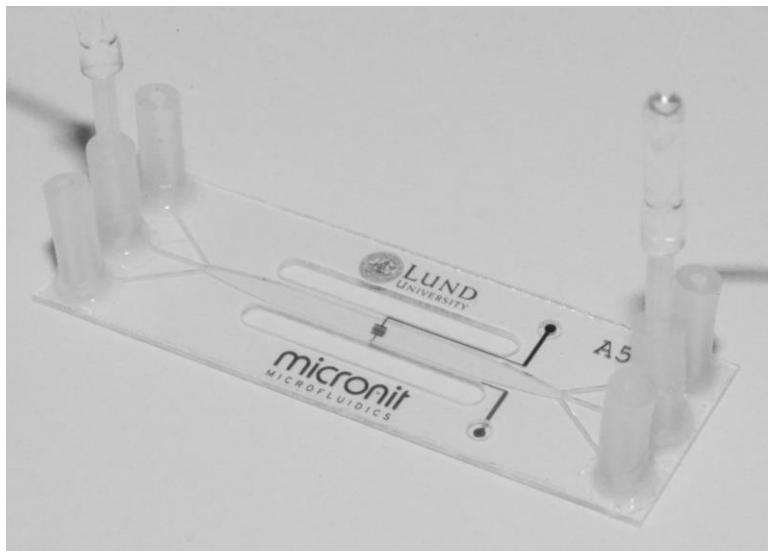

Figure 5.4. Image of the glass chip. The two circular metal areas to the right of the middle are the connection sites to the electrodes (electrode pads). One can be contacted from the top side of the chip and the other from the opposite side. In the middle of the channel the electrodes can be seen. At the right and left sides of the chip the three inlet and three outlet tubing are glued to the chip.

5.1.3 Resonator and transducer design

A version of the layered resonator shown in *Figure 4.5* has been used in this project. The thicknesses of the layers have not been perfectly matched to the frequencies used, i.e. they did not perfectly match the λ/2- and λ/4-criterions mentioned in *Section 4.2.1 Principles of acoustic trapping* and shown in *Figure 4.5*. Neither did the transducer have the recommended thickness of 0.84*λ/2 that was mentioned in *Section 4.2.4 Piezoelectric transducer*. However, since a kerfed transducer, see *Section 4.2.5 Kerfed transducer*, was used in this project, the thickness recommendation does not apply. The resonance frequency of the used transducer was around 4 MHz.

The transducer used in this thesis was soldered onto a printed circuit board (PCB). In *Figure 5.5* a schematic of the transducer and the PCB can be seen. The PCB had a hole in the middle, called air-backing, with the purpose of preventing acoustic energy to be transmitted away from the microfluidic

channel and to allow the crystal to oscillate freely. Length, width and height of the transducer used were 3.2 mm, 0.8 mm, and 0.4 mm, respectively. The material of the transducer was lead zirconate titanate (PZT) with hardness grade pz-26. It is a material often used for transducers intended for transmitting ultrasound; another hardness grade should be used when the purpose is to use it in an ultrasound receiver.

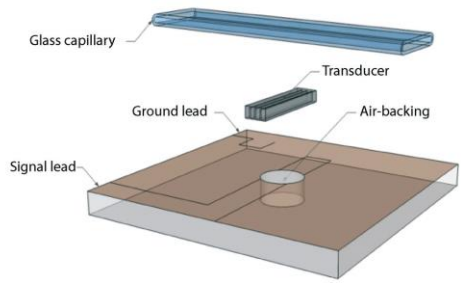

Figure 5.5. Schematic of the transducer and the PCB. The transducer is placed on top of the air-backing, and the glass chip (called glass capillary in image) is placed on top of the transducer and PCB. Reproduced from [13] with permission of The Royal Society of Chemistry.

5.1.4 Chip holder

Since the glass chips used in this project were very fragile, they were placed in a holder, which also was designed to make it more convenient to connect the chip to the impedance analyzer, and observe the chip under a microscope. The holder fixated the chip and the design allowed for connections to the tubing and the electrodes. A CNC mill (a computer-controlled mill) was used to fabricate the holder from aluminum. The holder consisted of four layers of aluminum chips that were screwed together, with the glass chip and transducer in between the two middle layers. The two upper layers had openings in the middle so that it was possible to observe the middle part of the channel in a microscope. The transducer was recessed into one of the inner aluminum chips with the glass chip placed on top, see *Figure 5.6*. Glycerol was applied as a coupling layer between the transducer and the glass chip to avoid gas bubbles or gas areas and to match the acoustic impedance, and thus enhance transmission of the ultrasonic waves into the channel. Wires and tubing were connected to the transducer and glass chip via drilled holes in the aluminum holder.

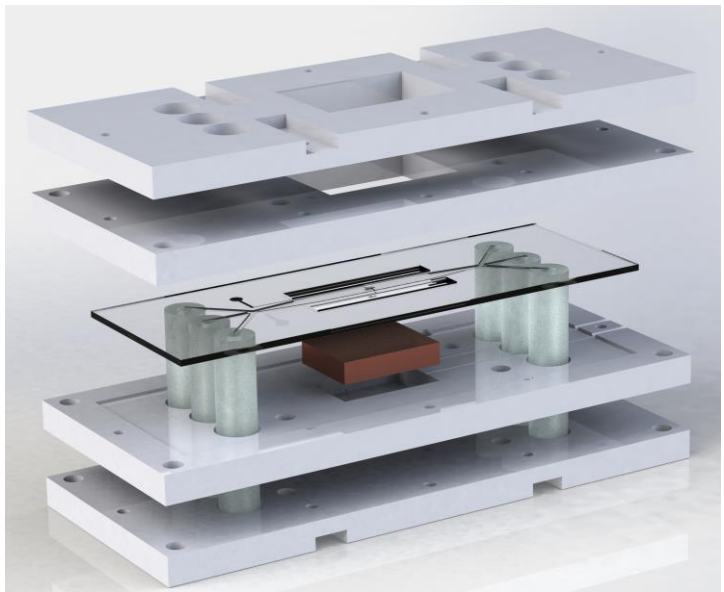

Figure 5.6. 3D-model of the chip holder with the glass chip and transducer in-between. The tubing connected to the glass chip go through drilled holes in two of the aluminum layers. The rectangular holes in the two top layers are enabling visual access to the trapping area of the chip. Image courtesy of Gustav Persson.

Pogo pins were used to contact the electrode pads on the glass chip. A pogo pin was soldered onto a custom-made PCB that then was screwed to the chip holder so that the pogo pin was pressed onto the electrode pad, see *Figure 5.7* and *Figure 5.8*. The outer aluminum chips were used mainly to keep the PCBs at the right distance from the glass chip so that the pogo pins could contact the electrode pads at the glass chip without breaking the electrodes. An SMA-contact was then soldered onto the PCB in order to be able to connect the chip to the impedance analyzer with BNC-cables, see *Figure 5.7*. In order to avoid electric noise the entire holder was grounded. A ground braid was soldered onto the grounded part of the SMA-contact and the other end was fastened to the aluminum holder, see *Figure 5.8*. When BNC-cables were connected to the SMA-contact, the holder became grounded relative to the impedance analyzer.

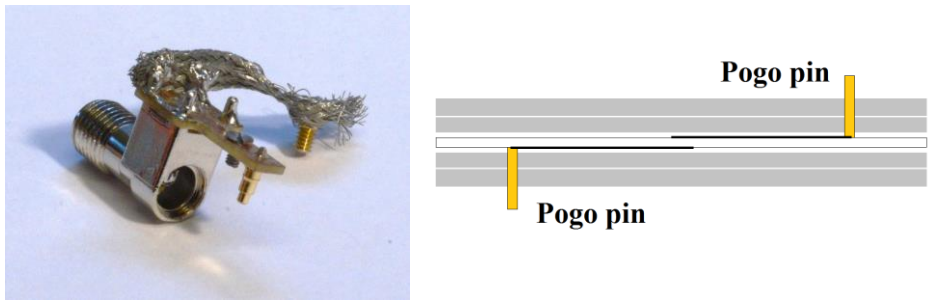

Figure 5.7. The left image shows the SMA-contact (with the screw thread), the attached PCB (the top flat structure), and the ground braid. The golden pin pointing downwards is the pogo pin that is used to contact the electrode pads on the glass chip. The right schematic pictures how the pogo pins contact the electrode pads on the glass chip through the aluminum holder. The white layer in the middle is the glass chip and the grey layers are the aluminum holder. The thicker larger black lines are the electrode pads and their wiring leading to the measuring area.

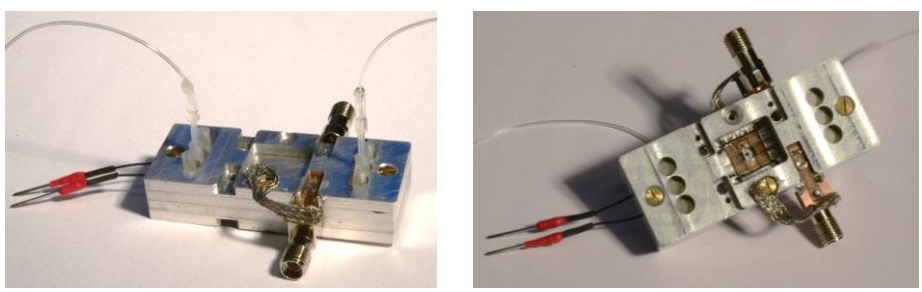

Figure 5.8. Images of the assembled chip holder containing the glass chip and transducer. The black and red wires to the left should be connected to a waveform generator to actuate the transducer. The two SMA-contacts are attached to the chip holder from the top and bottom. In the right image the channel is visible through the rectangular hole in the chip holder.

5.1.5 Frequency tracker

In order to find the resonance frequency of the resonating system, a frequency tracker was used. The tracker was custom-made by M. Evander and B. Hammarström [13]. It was connected to an arbitrary waveform generator, and was controlled through a LabVIEW® program. The resonance frequency was found by applying an AC-voltage to the transducer and simultaneously measuring the impedance over the transducer. A range of frequencies was tested and the resonance frequency was the one yielding the lowest impedance magnitude, hence highest power. Thereafter, the resonance frequency found was used to actuate the transducer with the waveform generator, i.e. the frequency tracker was only a tool to find the resonance frequency of the

system and was not continuously used during the trapping. See *Figure 5.9* for an example plot given by the resonance tracker.

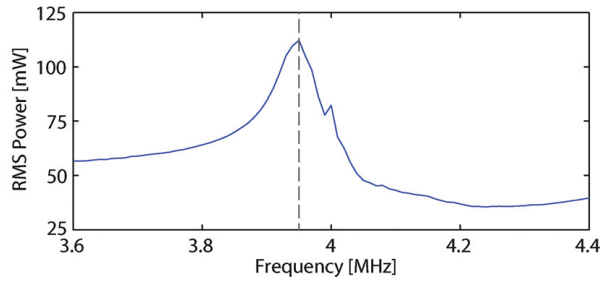

Figure 5.9. Frequency tracking spectrum. The resonance frequency is the one yielding the highest power. Reproduced from [13] with permission of The Royal Society of Chemistry.

5.2 Chemicals, buffers and cell suspensions

5.2.1 Particles in saline solution

To configure the acoustic trapping system, polystyrene particles of different sizes were used: 3 µm, 7 µm, 10 µm, and 12 µm (79166, 78462, 55463, 88511, Fluka, Sigma-Aldrich, St. Louis, MO) and silica particles with a diameter of 8 µm (GK1040001, Kisker, Steinfurt, Germany). The particles were suspended in 0.9% sodium chloride solution (S8776, Sigma-Aldrich, St. Louis, MO) since impedance spectroscopy requires an electrically conducting medium.

5.2.2 Tyrode's-HEPES-albumin buffer (TAB)

The buffer used for the platelet suspension was Tyrode's-HEPES-albumin buffer (TAB) consisting of 8 g/L NaCl, 200 mg/L KCl, 1 g/L $NaHCO_3$, 58 mg/L Na_2HPO_4, 203 mg/L $MgCl_2 \cdot 6H_2O$, 294 mg/L $CaCl_2 \cdot 2H_2O$, 1.19 g/L HEPES (4-(2-hydroxyethyl)-1-piperazineethanesulfonic acid) and 0.35% human serum albumin (HSA) at pH 7.35. The buffer was supplemented with 14% anticoagulant solution containing acid citrate dextrose (ACD) (C3821, Sigma-Aldrich, St. Louis, MO), 2 mM EDTA (ethylenediamine-tetraacetic acid), 0.1 µM PGE-1 (prostaglandin E_1), and 0.3 mM Aspirin.

5.2.3 Platelet-rich plasma (PRP)

For the platelet experiments, platelet-rich plasma (PRP) was used. Blood was collected from healthy volunteers using an intravenous catheter (BD Nexiva). 14% acid citrate dextrose (ACD) (C3821, Sigma-Aldrich, St. Louis, MO) was added to the blood to prevent platelet activation and coagulation. The first few mL of collected blood was discarded since it usually has higher concentrations of platelet activation factors, for example thrombin. The blood was placed in a water bath for 15 min at 37°C and subsequently centrifuged at $250 \times g$ for 15 min at 37°C. Approximately 85% of the PRP was aspirated from the centrifuged blood.

5.2.4 Thrombin receptor activating peptide (TRAP)

Thrombin receptor activating peptide (TRAP) (S1820, Sigma-Aldrich, St. Louis, MO) was used to activate the platelets. TRAP is a synthetic peptide that activates the thrombin receptor and has similar effects as thrombin, such as platelet aggregation and an increase in cytosolic calcium [34]. TRAP was dissolved in TAB buffer in order to maintain the electrical properties of the fluid in the channel after the TRAP-loaded buffer was inserted. TRAP concentrations of 20 µM and 40 µM were tested.

5.2.5 FITC-labeled CD62-P antibodies

Fluorescein isothiocyanate (FITC)-labeled CD62-P antibodies (561922, BD, Franklin Lakes, NJ) were used to label the platelets before FACS-experiments of the platelet activation level were carried out. FACS (fluorescence-activated cell sorting) is a type of flow cytometry that is used to sort and count cells with different antibody-affinity, in this case activated and non-activated platelets. CD62-P antibodies bind to activated platelets but not to non-activated. Hence, the number of activated platelets can be measured.

5.3 Experimental procedures

5.3.1 Acoustic trapping

Trapping was performed by infusing the objects (platelets or particles) into the channel with a syringe pump. An arbitrary waveform generator, which was connected to the transducer, was set to the resonance frequency found with the

frequency tracker. The resonance frequencies were 3.8–4.0 MHz and the voltage was set to 8 V_{pp} or 10 V_{pp} (peak to peak-value).

5.3.2 Impedance measurements

Impedance measurements were carried out with an impedance analyzer. The measurements were done by applying an alternating voltage at 400 evenly spread frequencies, ranging from 100 kHz to 15 MHz, with the impedance analyzer's oscillating level set to 0.3 V. This frequency sweep was made every two seconds and the current flowing between the electrodes in the channel was simultaneously measured. Thereby, the real and imaginary parts of the impedance could be calculated. The data was transferred from the memory of the impedance analyzer to a computer via a DAQ-cable (data acquisition-cable) and the magnitude and phase of the impedance were presented with respect to the frequency in MATLAB®.

5.3.3 System-related parameters affecting the impedance

In order to investigate how several possible parameters affected the impedance, experiments were made with different parts of the setup turned off and turned on; for example, the transducer and the syringe pump. These experiments were carried out with saline solution or TAB buffer in the channel, but without any particles. The effect of the voltage amplitude used to actuate the transducer was investigated by increasing the amplitude 1 V step by step from 1 V_{pp} to 10 V_{pp}. The temperature dependency of the system was studied by heating the whole setup with a heat gun without affecting the setup in any other way.

5.3.4 Particle and platelet measurements

The first experiments were conducted with polystyrene and silica particles in saline solution, since they could be used as simple cell models for characterization of the setup. The impedance measurements were mostly started before the ultrasound transducer and syringe pump were turned on to be able to compare the impact of the equipment to the impact of the particles captured in the acoustic trap. In order to let the system reach equilibrium and for the impedance to stabilize, no particles were inserted immediately after the transducer had been turned on. When the impedance had stabilized (after 30–100 seconds), either polystyrene or silica particles or platelets were introduced into the channel. Approximately 30 µL was introduced with flow rates of

10 or 20 µL/min. Since the measurements were started before the particles/cells were introduced into the system the whole progress of the particles/cells filling the trap was recorded.

Platelet activation was induced by infusing either 20 µM or 40 µM TRAP into the channel with a flow rate of 10 µL/min. The TAB-flow was substituted with continuously flowing TRAP-loaded TAB to maintain the activation and to avoid reversibility.

5.3.5 Control of platelet activation level with FACS

FACS tests were conducted to determine if the platelets were mechanically activated by the ultrasonic waves, see *Section 4.5.4 Shear stress-induced activation*, and to confirm that they were activated by 20 µM TRAP. Due to lack of time, the FACS-tests were performed using a different channel design than in the previous experiments with only one outlet, through which it was easier to extract the cluster. Three different samples were prepared for the FACS-evaluation. The flow rate was always set to 10 µL/min. For the first sample, platelets were inserted into the channel, trapped by the ultrasound, and then released into FACS-test tubes. FITC-labeled CD62-P antibodies were applied to the tube to stain the potentially activated platelets. A second plug of platelets were inserted into the channel and trapped. Antibodies were inserted while the platelets were kept in the acoustic trap, without insertion of TRAP. Finally, a third plug of platelets were captured in the trap and this time exposed to TRAP before the antibodies were inserted. All the test samples were run through the FACS and the number of activated platelets was counted.

6 Results and Discussion

6.1 Acoustic trapping

Both plastic and silica particles and platelets were successfully trapped at several different occasions. All the different sizes of the particles used were equally easy to trap. *Figure 6.1* shows trapped particles and platelets.

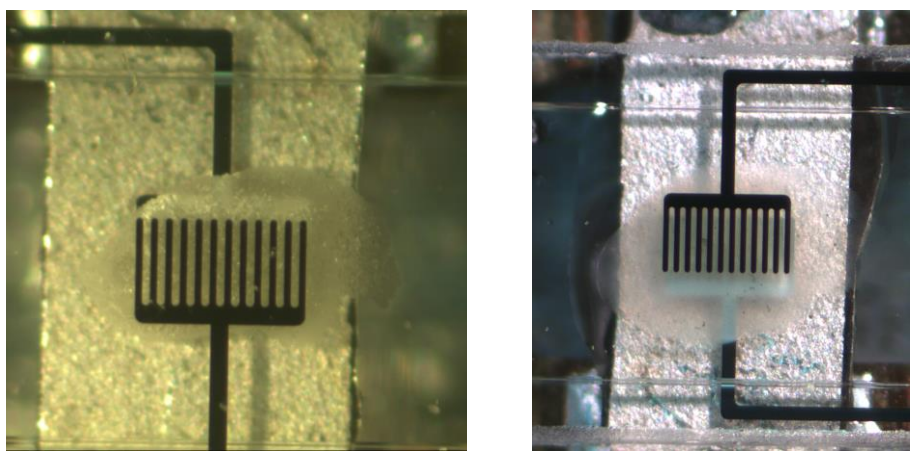

Figure 6.1. The left image shows trapped polystyrene particles and the right shows trapped platelets. The fingerlike structures are the electrodes and the large silver-colored rectangle is the transducer.

When the first particles were trapped, they aligned in a plane at the pressure node in the center of the channel and formed a monolayer, i.e. a layer that was only one particle diameter thick. As the cluster got larger, it formed more layers and the particles got more closely packed. It was visible that the cluster twitched as the particles changed confirmation. For all particles, and especially the platelets, it was hard to trap the very first that arrived to the trap. As the concentration increased, the trap started to gradually fill and usually no further trapping problems were observed. Furthermore, one could observe that the trapped platelets in the cluster had adhered to each other in some way, and therefore continued to stay together when the ultrasound had been turned off.

The problems with trapping the first particles were probably caused by the fact that the first particles and platelets arriving to the trapping area had a lower

concentration due to dispersion. The dispersion was mainly caused by the parabolic flow profile, see *Section 4.1.2 Parabolic flow profile*, which created a concentration gradient in the first part of the inserted platelet plug, with lower concentration at the front of the plug. Another phenomenon emerging in the channel was acoustic streaming. The acoustic fields caused the fluid to stream close to the trapping area and this sometimes pulled the particles/platelets away from the trap. Yet, if the amplitude of the voltage used to actuate the transducer was lowered, streaming deceased and trapping was easier accomplished. Therefore, a drive voltage amplitude of 8 V_{pp} was preferred over 10 V_{pp}.

Sometimes, it was difficult to fill the entire area between the electrodes, which were co-aligned with the trap. That was probably because too few particles were inserted into the channel or that they got stuck someway along the way from the syringe to the trap. When a sufficient amount of particles reached the trap, it was almost never any trouble to fill, and even overfill, the trap and to fill the area between the electrodes. Concerning the suspected adhesion, it was not clear what mechanism lay behind it. At least, it did not seem to be proper platelet aggregation, since the cluster could still change confirmation when it was pulled back to the trap when the ultrasound was turned off and on again.

6.2 Impedance measurements

Both the magnitude and the phase of the impedance were plotted against the frequency, see *Figure 6.2*. When measurements where performed on a TAB-buffer filled channel, the magnitude decreased rapidly in the lowest range of frequencies, leveled out in the middle range, and then dropped again in the highest range. The phase was recorded but was not used for any further analysis, both because lack of time and that the magnitude was more intuitively interpreted.

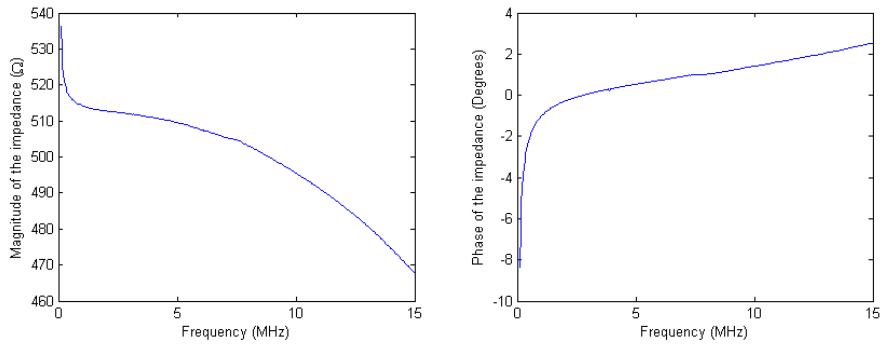

Figure 6.2. The diagram to the left shows an example of the magnitude of the impedance plotted against the frequency. The diagram to the right shows the corresponding phase of the impedance plotted against the frequency. In this particular case, the measurements were performed on a TAB-buffer filled channel.

6.3 Combination of acoustic trapping and impedance spectroscopy

6.3.1 System-related parameters affecting the impedance

The measured magnitude of the impedance in the system was seen to decrease when the ultrasound transducer was active, see *Figure 6.4*. The decrease was larger for a higher voltage amplitude used to actuate the transducer, see *Figure 6.3*. It was also observed that a flow rate increase resulted in an increase in the impedance magnitude, if the ultrasound transducer was active, see *Figure 6.4*. Heating of the channel with a heat gun also resulted in an impedance magnitude reduction, see *Figure 6.5*. All these changes were observed over the whole spectrum of frequencies utilized for the measurements (100 kHz–15 MHz). Additionally a minor impedance disturbance was detected at the frequency used to actuate the transducer.

Figure 6.3 shows a reduction in impedance magnitude due to an increase in voltage amplitude. It was observed that when the amplitude was increased by 1 V, the impedance magnitude decreased on average 3 Ω for all frequencies tested (100 kHz–15 MHz). Both *Figure 6.3* and *Figure 6.4* show that the impedance magnitude decreased approximately 30 Ω when the voltage amplitude was set to 10 V. As can be seen in *Figure 6.4*, the impedance magnitude decrease occurred immediately after the ultrasound was turned on and the impedance stabilized after around 30 seconds.

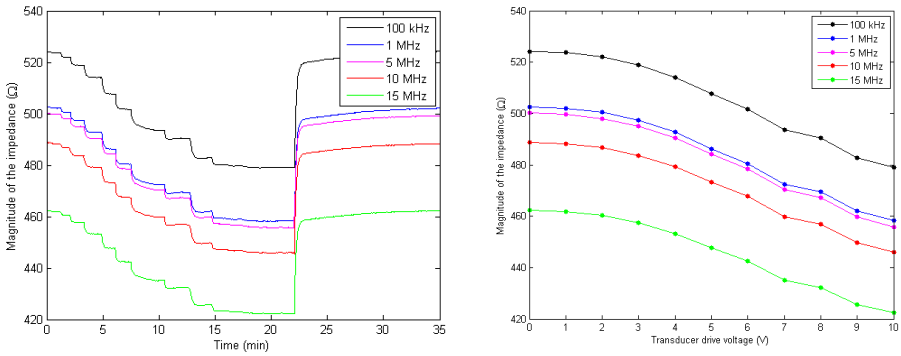

Figure 6.3. The diagram to the left shows a decrease in impedance magnitude when the amplitude of the voltage used to actuate the ultrasound transducer was increased. Each impedance magnitude reduction step correlates to an amplitude increase of 1 V. At 22 minutes the ultrasound was turned off. The diagram to the right shows the relation between magnitude of impedance and transducer drive voltage. The diagrams depict the impedance magnitude variation at five different measuring frequencies.

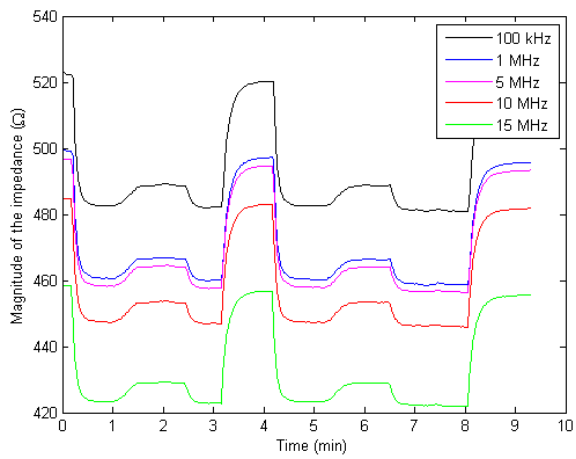

Figure 6.4. An impedance magnitude reduction caused by the ultrasound and fluid flow can be seen in this diagram. The decrease in impedance magnitude at 0 and 4.5 minutes was caused by the actuation of the ultrasound. When the fluid flow was turned on, at 1 and 5 minutes, the impedance magnitude increased. At 2.5 and 6.5 minutes the fluid flow was turned off and the impedance magnitude correspondingly decreased. The increase at 3 and 8 minutes was caused by the ultrasound being turned off. The diagram depicts the impedance magnitude variation at five different measuring frequencies.

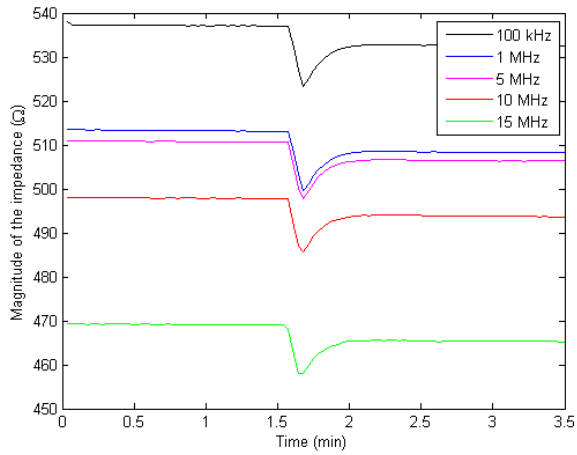

Figure 6.5. The diagram shows an impedance magnitude decrease in the channel caused by a temperature increase induced with a heat gun. At 1.5 minutes the heat gun was shortly turned on. The diagram depicts the impedance magnitude variation at five different measuring frequencies.

The impedance changes caused by both the ultrasound and the fluid flow were most probably due to temperature changes in the fluid. Due to energy losses in the ultrasound transducer, the transducer and consequently the fluid were heated up, which in turn resulted in an impedance magnitude decrease. When the fluid temperature in the measuring point was higher than the ambient temperature, the fluid flow caused the fluid temperature in the measuring point to drop, since the flowing fluid was colder than the fluid in the measuring point. The temperature decrease caused the impedance magnitude to increase. Hence, the increased fluid flow counteracted the temperature increase caused by the transducer. These changes correspond to the temperature dependency of the electrical conductivity in aqueous solutions. As the temperature in the solution is increased, the viscosity is decreased and that in turn increases the conductivity, i.e. lowers the impedance magnitude [35]. The temperature dependency has to be taken into account when using the system. Alternatively, some kind of cooling system, with the ability to keep the temperature stable, has to be developed.

The impedance disturbance at the frequency used to actuate the transducer might have been caused either by the voltage itself that was applied to the transducer, or by the standing waves that arose in the channel. No further investigation regarding the frequency disturbance was conducted, since it did not seem to influence the measurements in general.

6.3.2 Impedance measurements on particles

The impedance magnitude measured in a channel filled with saline solution was about 500–600 Ω. When polystyrene or silica particles were introduced into the channel and trapped between the electrodes by the acoustic waves, the impedance magnitude increased approximately 50 Ω over the whole spectrum of frequencies, see *Figure 6.6*. The reason for this was that the electrical resistivity of polystyrene and silica was higher than that of water.

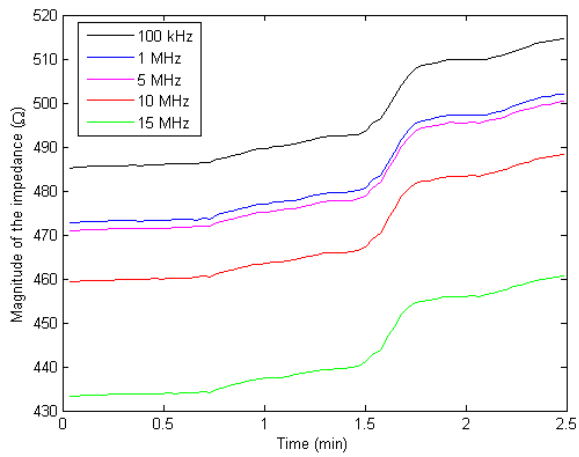

Figure 6.6. The diagram shows filling of the trap with polystyrene particles. After 1.5 minutes the electrodes were almost fully covered and therefore the largest increase occurred thereafter. The diagram depicts the impedance magnitude variation at five different measuring frequencies.

It was also observed that the increase in impedance magnitude was not linear to the filling of the trap; the largest part of the increase in impedance magnitude occurred when the last part of the electrodes was covered. The reason for this is not known, but due to this it was important, for the measurements performed in this thesis, to make sure that the area between the electrodes was completely filled before any further measurements could be performed.

When particles were trapped in the channel and the current flowed from one electrode to the other, it could mainly take three different paths; either through the particles, in the voids between the particles, or around the whole cluster. Both polystyrene and glass had several orders of magnitude higher resistivity than saline solution so it was rather unlikely that the current would go through the particles. Most likely, the current flowed through the cluster in the space between the particles. Thus, the increase in impedance magnitude could be

explained by the decrease in cross-sectional area that the current could flow through, i.e. the saline cross-sectional area between the electrodes.

6.3.3 Impedance measurements on platelets

Platelets were successfully trapped and the filling of the trap resulted in an impedance magnitude increase of 20–60 Ω, depending on the frequency, from around 500 Ω for an empty trap. The lower frequencies resulted in larger impedance magnitude increases, see *Figure 6.7*. Similarly to the particle experiments, filling of the trap had the largest impact when the last part of the electrodes was covered. Moreover, it was observed that the impedance magnitude decreased slightly after the trap had been completely filled.

As in the case with the particles, the impedance magnitude increase was probably due to the displacement of the buffer, which had lower electrical resistivity than the platelets. However, conversely to the case with the particles, it was possible for the current to flow through the platelets, but only at higher frequencies, see *Section 4.4 Cells in electrical fields*. This was probably the reason for why the impedance difference between a full and an empty trap differed between different frequencies.

The impedance magnitude decrease that occurred after the trap was filled was probably due to plasma being washed away and replaced with TAB buffer.

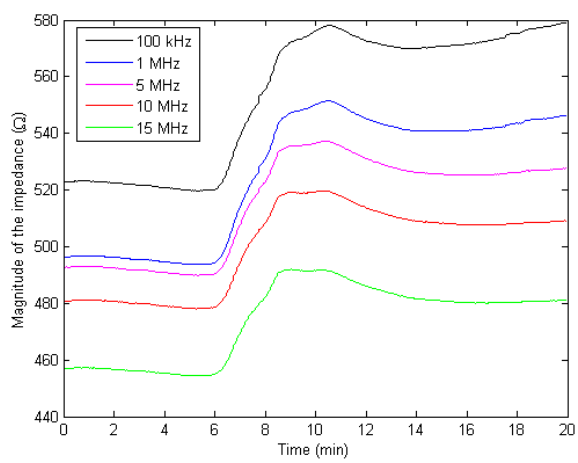

Figure 6.7. An impedance magnitude increase caused by platelet filling of the trap can be seen in the diagram. The total increase varied for different frequencies. Lower frequencies showed a larger increase. The diagram depicts the impedance magnitude variation at five different measuring frequencies.

6.3.4 Difference between activated and non-activated platelets

The insertion of TRAP over the trapped platelets resulted in an impedance magnitude decrease; the reduction was most probably due to a platelet reaction caused by TRAP. At a TRAP concentration of 20 µM an initial impedance magnitude decrease of 4–15 Ω was observed over the frequency spectrum, whereas for 40 µM the initial change was 8–25 Ω and the sustained decrease was 5–15 Ω, see *Figure 6.8* and *Figure 6.9*.

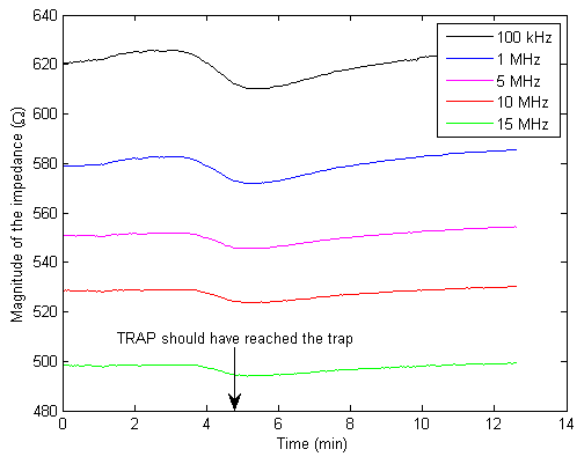

Figure 6.8. The diagram shows an impedance magnitude decrease caused by 20 µM TRAP. The arrow indicates when TRAP should have reached the trapped platelets. It can clearly be seen that the decrease is more prevalent at lower frequencies. The diagram depicts the impedance magnitude variation at five different measuring frequencies

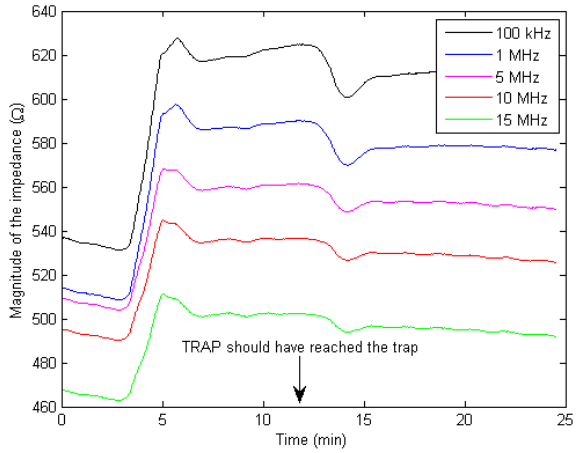

Figure 6.9. The diagram shows filling of a trap with platelets and the reaction to 40 µM TRAP. The impedance magnitude increase caused by the filling can be seen from 3 to 5 minutes. The arrow indicates when TRAP should have reached the platelet cluster in the trap. Approximately 2 minutes later an impedance magnitude decrease was observed. The diagram depicts the impedance magnitude variation at five different measuring frequencies.

To ensure that the impedance magnitude decrease was not due to the insertion of the agonist itself, an impedance comparison between TAB with and without added TRAP was conducted. This comparison showed no significant difference between the two solutions, at least not compared to the impedance magnitude change observed when platelets were present, see *Figure 6.10*. Hence, the impedance change was probably due to some kind of platelet reaction, which was also confirmed by the activation control experiments performed with FACS, see *Section 6.3.5 Control of platelets activation level with FACS*. Two possible reasons for the impedance magnitude decrease are ion release and shape change. Messenger molecules are released from activated platelets to enhance activation of surrounding platelets. Some of these molecules are charged and should therefore lower the impedance magnitude between the electrodes in the channel. If the trapped platelets changed shape, the voids between the platelets might also have changed and affected the current flowing through the cluster. It is not clear whether the shape change should lead to an increase or decrease in impedance magnitude. If new voids, through which the current could flow, were formed in the cluster, the impedance magnitude should decrease. On the other hand, if the platelets got closer packed and the cluster got bulkier, the impedance magnitude should increase.

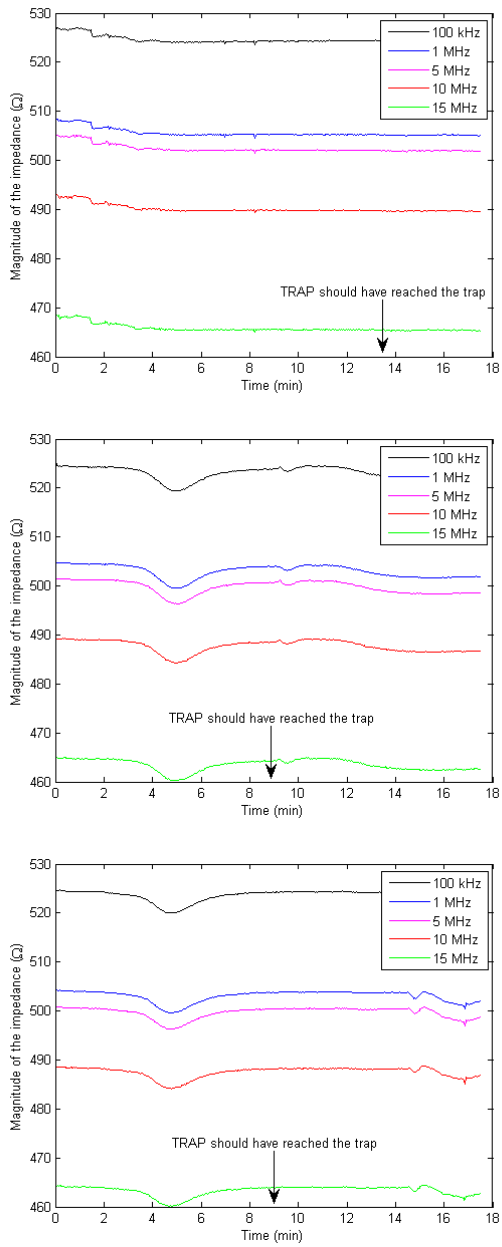

Figure 6.10. The three diagrams show the magnitude of the impedance as the solution in the channel was changed from pure TAB to TAB-diluted TRAP when no platelets were present. The arrows indicate the time when the TRAP was calculated to reach the measuring point. No significant impedance change can be seen at that time. However, small impedance changes were observed in two of the measurements (the two bottom diagrams) before the TRAP should have reached the measuring point. This was most likely not due to TRAP, but some other disturbance.

One of the main objectives of the thesis, see *Chapter 2 Main objectives of the thesis*, was to identify frequencies where the impedance differed significantly between activated and non-activated platelets. The experiments showed that at lower frequencies, up to approximately a few megahertz, impedance changes were more easily detected than at higher frequencies. On the other hand, the system was more sensitive to impedance disturbances at lower frequencies. Disturbances might lead to misinterpretation of the data, for example, if the activation of the platelets and the disturbance coincide, one might overlook the fact that the platelets have been activated. Likewise, a change in impedance due to disturbance might be misinterpreted as platelet activation.

Due to relatively low flow rates during the experiments (10 µL/min) it was hard to tell exactly when TRAP had reached the trapped platelets. However, relatively good estimations were done by calculating the time needed for TRAP to be transported from the valve to the trapped platelet plug. However, the fact that the flow rate in the middle of the channel was higher than that at the sides was disregarded. The TRAP experiments were performed several times at two different occasions, and an impedance magnitude decrease was detected at most of the measurements.

6.3.5 Control of platelet activation level with FACS

FACS-tests showed that the platelets probably were activated by the ultrasound but significantly more activated when exposed to TRAP. The level of activation depended on how the FACS was calibrated. When an unstained sample was set to fluoresce at 1%, a non-activated sample showed approximately 15% fluorescence and an activated sample 60%, see *Table 6.1*.

	Unstained platelets	Non-activated platelets	Activated platelets
Fluorescent platelets (%)	1	15	60

Table 6.1. Results from FACS-measurements of platelet activation level. The fluorescently labeled antibodies used did only bind to activated platelets; therefore, the number of activated platelets could be calculated from the fluorescence.

First of all, one must remember that only one test was run and the possible error sources were many. With that said, the FACS-test showed promising results and, at the same time, encouraged further testing. The two most striking aspects of the results were the relatively high level of activated platelets in the sample to which no TRAP had been added, and the relatively low level of

activation in the TRAP-exposed sample. The first aspect is perhaps caused by shear stress-induced activation either by the ultrasonic waves or by the PRP preparation procedure. To investigate the ultrasound's impact on the activation level, one sample should be prepared with platelets that have been inserted into the channel when the ultrasound is turned off. In addition, one sample with platelets that have not been inserted into the channel at all should be compared. When blood is gathered from a patient, it is usually assumed that about 5% of the platelets become activated due to the blood sampling procedure. When the blood was centrifuged and processed in the lab to prepare PRP even more platelets might have been activated. This could maybe be examined by handling the blood as carefully as possible and using more gentle spinning protocols, and comparing the activation level to the 15% yielded in this study. The second aspect, i.e. the relatively low level of activation in the TRAP-exposed sample, could be studied by increasing the concentration of TRAP, which could lead to a higher activation level, as long as not all the platelets are activated.

7 Conclusions

The results presented in this report show that the two techniques of acoustic trapping and impedance spectroscopy can be combined for simultaneous contactless immobilization and impedance measurements of micrometer-sized objects in a microfluidic channel. Additionally, the experiments showed that it is possible to measure impedance differences between clusters of activated and non-activated platelets. Furthermore, the FACS-analysis indicated that the platelets are not to a large extent being activated by the acoustic field in the trapping point. It was also seen that the ultrasound and fluid flow affect the fluid temperature that in turn changes the impedance. Further developments of the system could lead to a well-functioning analysis system, for example for platelets, that could be used both within research and as a device for diagnostics.

8 Future prospects

Currently available platelet analysis techniques are labor intensive and time consuming. The technique presented here has several advantages to available techniques, for example it requires no pipetting and the sample does not have to go through several pre-treatment and analysis steps. Additionally, if several channels or trapping areas would be implemented it would allow for simultaneous analysis of multiple samples. Different tests could also be performed concurrently but separated from each other. Consequently, the setup has great potential to be developed to a fully automated analysis system.

A further advantage of the system is the possibility to implement it within different analysis fields, not only within platelet measurements. It could probably be used for measurements on other blood components and maybe even other cells and tissues. Another potential field of application would be drug research; immobilization of a cell culture enables studies on the reaction to certain drugs and drug concentrations over time. This would also reduce the need for laboratory animals.

However, several potential areas of improvements exist for the setup and further tests have to be performed. First, a weakness of the system today is the instability of the measured impedance. It is important that the impedance changes only when there is a change of the trapped cluster of platelets and not because of other disturbances in the system. One way to correct for this would be to use a third electrode as a reference electrode in the fluid, since it would allow for differential measurements. However, the whole system is quite sensitive and very easily affected by disturbances. Therefore, it is strongly recommended to improve the way the chip and equipment are assembled.

Second, the visual contrast between the trapped platelets and the background was very poor, it was sometimes hard to recognize whether the trap was full or not. This problem could be eliminated by covering the backside of the chip with a metal layer.

Third, the platelets' reactions to the system and also to insertion of agonists into the channel have to be further investigated. The FACS-analysis has to be repeated, and further tests, for example histology screenings and viability tests with trypan blue, are also recommended.

Last, it is desirable to be able to more precisely control the number of platelets being trapped. This, perhaps, can be realized by inserting them closer to the

trapping area. It would reduce the risk of the platelets being obstructed somewhere in the system during the insertion and from being dispersed.

To conclude, the first studies conducted on the system were promising although there are several weaknesses in the setup design and experimental procedure. The combination of acoustic trapping and impedance spectroscopy shows great potential for the future.

9 Popular science summary (Swedish)

Blodanalys på ett chip

På sjukhus och inom forskning görs dagligen mängder med analyser av till exempel blodprover, livsmedel och vattenprover. Analysmaskinerna kräver ofta relativt stora volymer av de vätskor som ska undersökas, men också av de reagenser som måste tillsättas för att analysen ska kunna genomföras. Dessutom måste proverna ofta förberedas i flera steg för att man ska kunna analysera dem, vilket är tidskrävande och kräver mycket personal och laboratorieutrustning. Detta är några av anledningarna till varför miniatyriserade laboratorium, så kallade Lab-on-a-chip, har blivit ett viktigt forskningsområde. Målet är att man ska kunna genomföra alla förberedelse- och analyssteg på ett chip som är mindre än en handflata i storlek och som har små inbyggda vätskekanaler. På så sätt behövs mindre vätskevolymer och mindre arbete från laboratoriepersonal.

I chipet kan man injicera olika sorters vätskor och analysera dem på flera sätt.

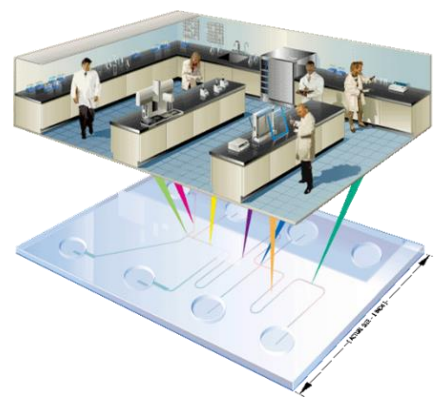

Illustration av Lab-on-a-chip. Genom att integrera flera analyssteg på ett litet chip, inte större än en handflata, hoppas forskarna kunna göra laboratorieanalyser smidigare och effektivare. Källa: www.gene-quantification.de/lab-on-chip.html

Elektriska mätningar är en sorts analysmetod som kan användas för att få information om ett prov, till exempel ett blodprov. Genom att leda ström genom blodet och mäta motståndet är det möjligt att ta reda på formen hos de celler som finns i blodet, olika form ger för det mesta olika motstånd. Ofta hänger formen ihop med

funktionen och genom att mäta hur cellerna ser ut kan man få reda på om de fungerar som de ska. Det är viktigt att kunna få information om cellernas funktion eftersom det också kan ge information om sjukdomar.

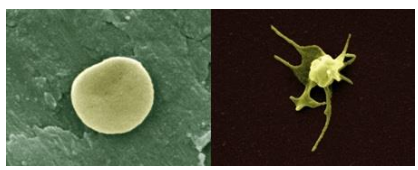

Bilder på blodplättar, som är en typ av blodceller. Bilderna visar blodplättar i olika stadier. Bilder tillhandahållna av M.D. David Erlinge, vid kardiologiska avdelningen på Skånes universitetssjukhus.

Vid vissa undersökningar av celler som flyter omkring i ett blodprov krävs en teknik för att hålla fast cellerna. En sådan teknik är akustisk infångning, vilken använder sig av ultraljud för att fånga och hålla fast objekt i en vätska, till exempel blodceller. Vanligtvis används ultraljud för att undersöka fostret på gravida kvinnor eller organ inne i kroppen. Men ultraljud har alltså fler användningsområden. Möjligheten att använda det för att fånga celler i en vätska beror på att ultraljudet utövar krafter på cellerna och på så sätt håller fast dem, utan direkt fysisk kontakt. Tack vare detta minskas risken att cellerna skadas. Tekniken fungerar också om vätskan runt omkring cellerna är i rörelse; vätskan flyter då förbi cellerna utan att de följer med i flödet.

På Lunds tekniska högskola har man nu lyckats kombinera akustisk infångning med elektriska mätningar. Mätningarna genomförs på ett chip som är 5 cm långt, 2 cm brett och 1 mm tjockt.

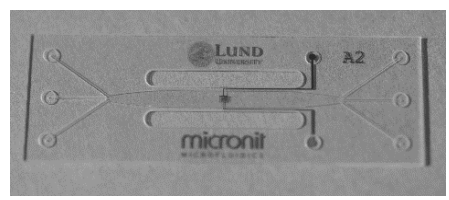

Det chip som används för mätningar på blodplättar vid Lunds universitet. Storleken på chipet är 5cm x 2 cm x 1 mm.

Det har visat sig vara möjligt att fånga en grupp blodplättar, en specifik typ av blodceller, och sedan mäta elektriskt på dem. Denna typ av mätning skulle i framtiden kunna komma att användas för att ta reda på om en patient har risk för åderförkalkning eller lider av blödarsjuka.

Carl Johannesson och Ellen Persson, **Institutionen för Biomedicinsk teknik, Lunds tekniska högskola. 2014-08-11**

10 References

1. Lenshof, A., et al., *Acoustofluidics 5: Building microfluidic acoustic resonators.* Lab on a Chip, 2012. **12**(4): p. 684-695.

2. Nilsson, J., et al., *Review of cell and particle trapping in microfluidic systems.* Analytica Chimica Acta, 2009. **649**(2): p. 141-157.

3. Folch, A., *Introduction to BioMEMS*. 2012, Taylor & Francis. p. 98-103.

4. Wikimedia. [Accessed 2014-07-02]; Available from: http://commons.wikimedia.org/wiki/File:Laminar_and_turbulent_flows.svg.

5. Bruus, H., *Theoretical Microfluidics*. 2008, OUP Oxford. p. 60-63.

6. Evander, M. and J. Nilsson, *Acoustofluidics 20: Applications in acoustic trapping.* Lab on a Chip, 2012. **12**(22): p. 4667-4676.

7. Hammarström, B., et al., *Non-contact acoustic cell trapping in disposable glass capillaries.* Lab on a Chip, 2010. **10**(17): p. 2251-2257.

8. Nilsson, A., et al., *Acoustic control of suspended particles in micro fluidic chips.* Lab on a Chip, 2004. **4**(2): p. 131-135.

9. Evander, M., et al., *Acoustophoresis in wet-etched glass chips.* Analytical Chemistry, 2008. **80**(13): p. 5178-5185.

10. Glynne-Jones, P., R.J. Boltryk, and M. Hill, *Acoustofluidics 9: Modelling and applications of planar resonant devices for acoustic particle manipulation.* Lab on a chip, 2012. **12**(8): p. 1417-1426.

11. Hammarström, B., *Acoustic Trapping in Biomedical Research*, in *Department of Biomedical Engineering Faculty of Engineering*. 2014, Lund University.

12. Laurell, T., F. Petersson, and A. Nilsson, *Chip integrated strategies for acoustic separation and manipulation of cells and particles.* Chem Soc Rev, 2007. **36**(3): p. 492-506.

13. Hammarström, B., et al., *Frequency tracking in acoustic trapping for improved performance stability and system surveillance.* Lab on a Chip, 2014. **14**(5): p. 1005-1013.

14. Bushberg, J.T., et al., *The Essential Physics of Medical Imaging*. 2011: Wolters Kluwer Health.

15. Dual, J., et al., *Acoustofluidics 6: Experimental characterization of ultrasonic particle manipulation devices.* Lab on a Chip, 2012. **12**(5): p. 852-862.

16. Kennelly, A.E., *Impedance.* American Institute of Electrical Engineers, 1893. **X**: p. 172-232.

17. Barsoukov, E. and J.R. Macdonald, *Impedance spectroscopy : theory, experiment, and applications / edited by Evgenij Barsoukov, J. Ross Macdonald*. 2005: Hoboken, N.J. : Wiley-Interscience, cop. 2005 2. ed.

18. Wikimedia. [Accessed 2014-07-15]; Available from: http://commons.wikimedia.org/wiki/File:Complex_Impedance.svg.

19. Cole, K.S., *Membranes, Ions, and Impulses: A Chapter of Classical Biophysics*. 1968: University of California Press.

20. Holder, D.S., *Electrical Impedance Tomography: Methods, History and Applications*. 2004: Taylor & Francis.

21. Cheung, K., S. Gawad, and P. Renaud, *Impedance spectroscopy flow cytometry: On-chip label-free cell differentiation.* Cytometry Part A, 2005. **65A**(2): p. 124-132.

22. Grimnes, S. and Ø.G. Martinsen. *Alpha-dispersion in human tissue*. 2010. Place of Publication: Gainesville, FL, USA. Country of Publication: UK.: IOP Publishing Ltd.

23. Guyton, A.C. and J.E. Hall, *Textbook of Medical Physiology*. 2010, Elsevier Saunders. p. 648-654.

24. Evander, M., et al., *Microfluidic impedance cytometer for platelet analysis.* Lab on a Chip, 2013. **13**(4): p. 722-729.

25. Picker, S.M., *In-vitro assessment of platelet function.* Transfusion and Apheresis Science, 2011. **44**(3): p. 305-319.

26. Hoffbrand, V. and P. Moss, *Essential Haematology*. 2011, Wiley. p. 315-328.

27. George, J.N., *Platelets.* Lancet, 2000. **355**(9214): p. 1531.

28. Jackson, S.P., *The growing complexity of platelet aggregation.* Blood, 2007. **109**(12): p. 5087-5095.

29. Breddin, H.K., *Can platelet aggregometry be standardized?* Platelets, 2005. **16**(3/4): p. 151-158.

30. Lu, Q., et al., *In Vitro Shear Stress-Induced Platelet Activation: Sensitivity of Human and Bovine Blood.* Artificial Organs, 2013. **37**(10): p. 894-903.

31. Hoffbrand, A.V., et al., *Postgraduate Haematology*. 2011: Wiley.

32. Michelson, A.D., et al., *Platelets*. 2007: Burlington : Academic Press 2007.

33. Tsiara, S., et al., *Platelets as predictors of vascular risk: is there a practical index of platelet activity?* Clin Appl Thromb Hemost, 2003. **9**(3): p. 177-190.

34. Landesberg, R., et al., *Activation of platelet-rich plasma using thrombin receptor agonist peptide.* Journal of Oral and Maxillofacial Surgery, 2005. **63**(4): p. 529-535.

35. Miller, R.L., W.L. Bradford, and N.E. Peters, *Specific conductance; theoretical considerations and application to analytical quality control*. 1988, U. S. Geological Survey: Reston, VA, United States: United States.